Preferential growth of thin rutile TiO$_2$ films upon thermal oxidation of sputtered Ti films

Chu-Chi Ting[a], San-Yuan Chen[a,*], Dean-Mo Liu[b]

[a]Department of Materials Science and Engineering, National Chiao-Tung University Hsinchu 300, Taiwan, ROC
[b]Department of Metals and Materials Engineering The University of British Columbia Vancouver, British Columbia V6T 1Z4, Canada

Abstract

Thin rutile TiO$_2$ films with (200) preferred orientation were fabricated by thermal oxidation of sputtered Ti metal films on a fused silica substrate. Experimental results indicate that the preferential crystal growth of (200)-oriented TiO$_2$ is determined by the competition between surface free energy and strain energy. The highly crystalline Ti film with (002) orientation has a greater tendency to promote the growth of (200)-oriented TiO$_2$. However, for the amorphous and low crystalline Ti films, orientation of the crystallites evolved in the resulting TiO$_2$ film tends to be randomly distributed. The extent of preferential crystal growth of TiO$_2$ (200) plane can be enhanced by decreasing the annealing temperature or the thickness of Ti film. © 2002 Elsevier Science B.V. All rights reserved.

1. Introduction

Control of preferential growth of a specific crystal plane within a film matrix allows the final properties such as optical, mechanical and electrical properties of the film to be manipulated in such a manner that further improves applications [1–3]. In general, the crystal plane with the highest atomic density exhibits the lowest surface free energy that favors a subsequent preferential growth. Preferential crystal growth, on the other hand, is also strongly dominated by the synthesis parameters or lattice mismatch between film materials and substrates. For instance, (004)-oriented anatase TiO$_2$ films fabricated from reactive sputtering process can be obtained by the control of substrate temperature or O$_2$ partial pressure [4]. Rutile TiO$_2$ films prepared by ion beam-assisted deposition can grow preferentially with (100), (101) or (002) orientation depending on the

impact angle and arrival ratio of ions to deposited atoms (i.e. I/A ratio) [5,6]. By applying a sol–gel spin-coating method, (004)-oriented anatase or (101)-oriented rutile TiO$_2$ films can be obtained through the selection of precursors and chelating agents [7]. In addition, (100)-oriented rutile TiO$_2$ and (001)-oriented Ti$_2$O$_3$ films can be grown epitaxially on (001)-oriented α-Al$_2$O$_3$ substrates because TiO$_2$ or Ti$_2$O$_3$ crystals have nearly identical hexagonal close-packed oxygen sublattices to the one of α-Al$_2$O$_3$ [8,9].

Thin TiO$_2$ films can be synthesized by several methods including sol–gel processing, reactive magnetron sputtering, spray pyrolysis, and plasma enhanced chemical vapor deposition (PECVD) [10–14]. In addition to the afore-mentioned synthetic schemes, previous investigation showed that the thermal oxidation of sputtered titanium metal film was found to be a rather simple technique to prepare TiO$_2$ thin films [15], which is also adopted in this work. It was found that the formation of (200)-oriented or disoriented rutile TiO$_2$ films depend on the crystallinity and orientation of Ti films initially prepared. The mechanisms affecting the preferred ori-

* Corresponding author. Tel.: +886-3-573-1818; fax: +886-3-572-4727.

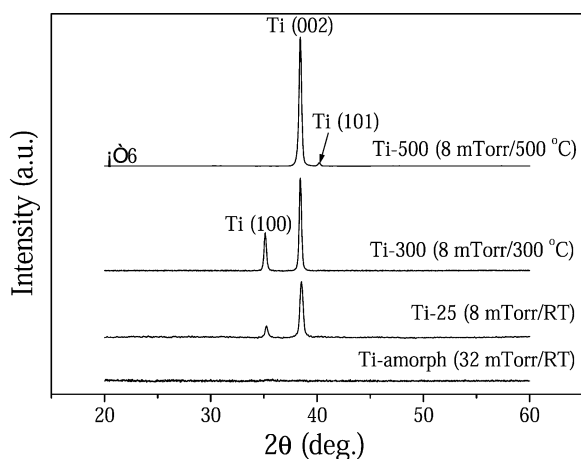*E-mail address:* sychen@cc.nctu.edu.tw (S.-Y. Chen).

Fig. 1. XRD patterns of sputtered Ti films deposited at different working pressures/substrate temperatures.

entation of resultant TiO_2 films during film growth will be discussed.

2. Experimental procedure

2.1. Film process

Titanium films were prepared using a d.c. magnetron sputtering system having a 30-dm³ cylindrical stainless-steel chamber with a base pressure of 5×10^{-6} torr. The target was a 3-inch-diameter titanium disk of 99.6% purity. Titanium was deposited at a constant d.c. power of 50 W onto a fused silica substrate. The target–

substrate distance was kept at 70 mm. The sputtering time was 30 and 40 min under a working pressure of 8 and 32 mtorr, respectively, in order to achieve the identical thickness of ~400 nm. The substrate temperatures were controlled at room temperature (RT), 300 and 500 °C. Ultra-high purity (99.999%) Ar gas was used for sputter-deposition. Prior to Ti deposition, the target was pre-sputtered in an argon atmosphere for 8 min in order to remove surface oxides on the target. Finally, the sputtered Ti films were subjected to post-deposition annealing at temperatures ranging from 550 to 1000 °C for 1 h in air.

2.2. Film characterization

The crystal structure was determined by X-ray diffractometry (MAC Science, M18X). The thickness of the Ti films and resultant TiO_2 films were measured using a surface profilometer (Sloan, Dektak³ST). Scanning electron microscopy (SEM; Hitachi, S4000) was used for microstructural examination.

3. Results and discussion

Fig. 1 shows the X-ray diffraction (XRD) patterns of the sputtered Ti thin films prepared at different working pressures/substrate temperatures (e.g. Ti-500 was denoted as the sputtering parameters of 8 mtorr/500 °C). The diffraction peaks, i.e. (002), (100) and (101) are characteristic of α-Ti. A decrease in sputtering pressure and an increase of substrate temperature markedly improve the crystallinity of resultant Ti films. Fig.
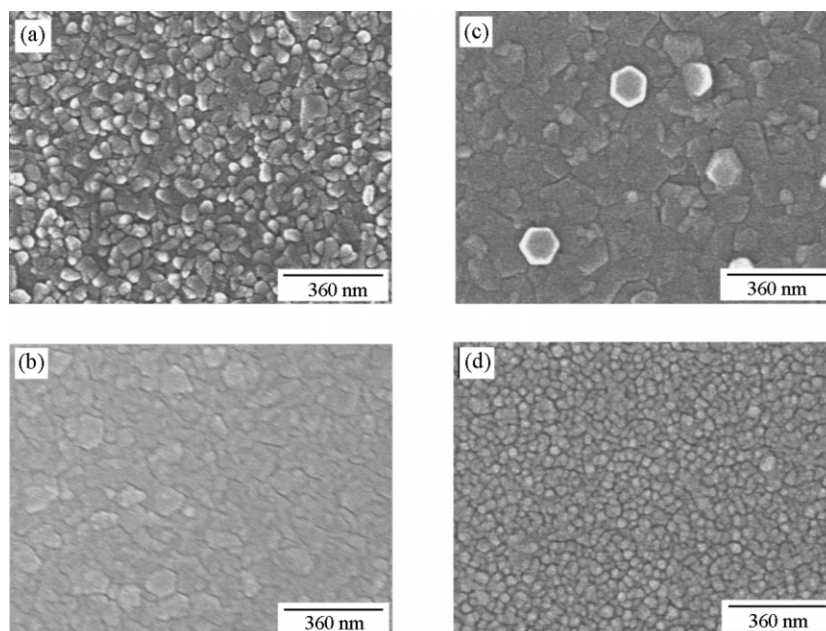

Fig. 2. The SEM photographs of sputtered Ti films deposited at different working pressure/substrate temperatures: (a) 8 mtorr/RT; (b) 8 mtorr/300 °C; (c) 8 mtorr/500 °C; and (d) 32 mtorr/RT.

2 shows scanning electron microscopy (SEM) photographs of the sputtered Ti films, where the Ti film deposited at 8 mtorr/500 °C exhibited surface morphology with large grain size and a few flat hexagonal crystal grains, whilst for those prepared at 32 mtorr/RT give rise to a fine-grained microstructure.

These results indicate that improved crystallinity and large grains were obtained at higher growth temperature and lower sputtering pressures. At 500 °C, the Ti film exhibits strong (001) preferred orientation, which is expected from surface free energy consideration. However, amorphous structure was observed when the deposition was performed at 32 mtorr/RT. This is due to reduced adatom mobility at lower substrate temperature, associated with decreased kinetic energy of arriving species because of collisions with residual gas molecules.

Before further discussion, it should be pointed out that this oxidation process involves growth of the TiO_2 crystals from the Ti/air interface (i.e. the portions of Ti atoms first exposed to oxygen) to Ti/substrate interface (i.e. 'downward growth'), rather than those growing 'upwards' from a 'bare' substrate by direct deposition methods [4–14]. Therefore, growth of the TiO_2 crystals depends solely on the movement of the TiO_2–Ti interface [16–18].

After thermal oxidation of the sputtered Ti films at 800 °C for 1 h, a typical rutile TiO_2 structure was developed as identified by XRD patterns in Fig. 3 [19]. Surprisingly, no anatase TiO_2 was detected over the entire annealing temperature range (550–1000 °C) of study. This phenomenon appears to be attributed to the formation of a large quantity of oxygen vacancies in the oxide film that is known to significantly accelerate the phase transformation of anatase to rutile, as further evidenced in previous work [15].

A randomly oriented rutile TiO_2 film was formed for Ti-25 films. However, preferred orientation along the TiO_2 (200) plane was developed from the starting Ti-500 film, having the highest degree (sharpest reflection peaks) of crystallinity among all the Ti films prepared. In other words, (200)-oriented TiO_2 film can be induced on the Ti films with (002) preferred orientation. These experimental observations strongly suggest a competition between two driving forces, i.e. surface free energy and strain energy effects, on determining preferential growth of the resultant TiO_2 crystals. The surface morphology of TiO_2 films grown from the thermal oxidation of Ti-500 film at 800–1000 °C for 1 h are shown in Fig. 4, where the grain size is increased from ~100 to ~180 nm after annealing at 800 and 1000 °C, respectively.

Numerous published reports have indicated that the metal and its oxide (e.g. TiO_2/Ti, ZrO_2/Zr, Cu_2O/Cu, MoO_3/Mo and Al_2O_3/Al) display the characteristics of oxidation anisotropy [20–25]. This phenomenon is
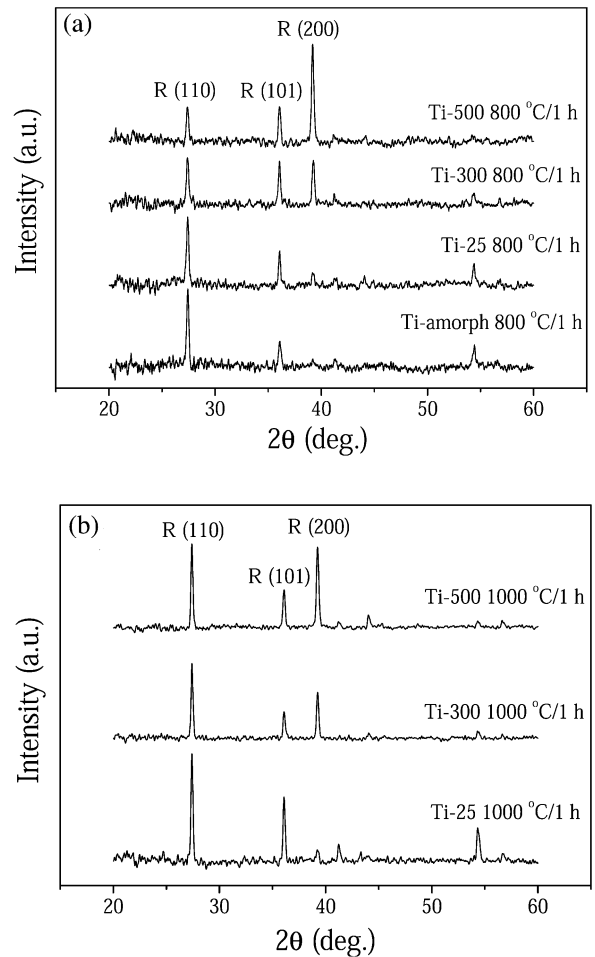

Fig. 3. XRD patterns of as-deposited Ti films with different sputtering conditions after thermal oxidation at (a) 800, and (b) 1000 °C for 1 h in air.

attributed to the epitaxial growth of metal oxide on parent metal. For example, Flower et al. used the transmission electron microscope to investigate the behavior of in situ oxidation reaction of α-titanium foil [20]. They found that rutile TiO_2 can easily grow epitaxially on a clean, electro-polished Ti surface [i.e. TiO_2 (100)//Ti (001) and TiO_2 (100)//Ti (100)], but those contaminated Ti grains will induce polycrystalline rutile TiO_2. As schematically illustrated in Fig. 5 for the atomic structures of some planes in rutile TiO_2 and α-Ti, the most favorable matching occurs at the TiO_2 (100)–Ti (100) interface. However, the lattice misfits between TiO_2 (100) and Ti (001) is as much as ~10% along the c-axis. Likewise, the ZrO_2/Zr system also exhibits epitaxial relationship, for instance ZrO_2 (−101)//Zr (100) and ZrO_2 (001)//Zr (001) [21].

The XRD patterns of Ti-25 and Ti-500 films oxidized at low temperatures for different time frames were shown in Fig. 6. Obviously, the Ti (002) peak gradually shifts towards low angles (from 38.41 to 37.11°) by increasing the oxidation time, and a similar observation
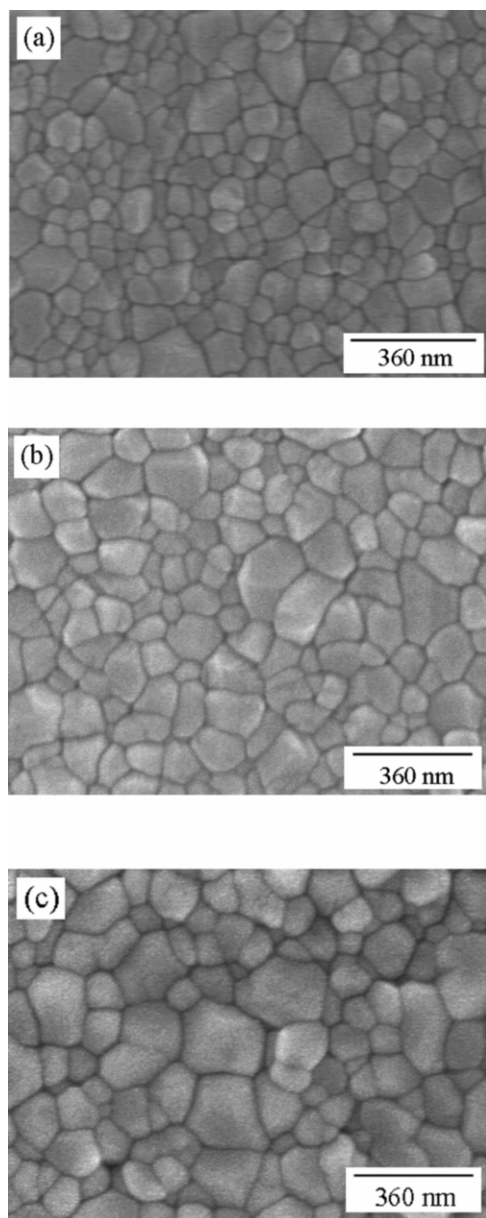
Fig. 4. The SEM photographs of TiO₂ films fabricated by thermal oxidation of Ti-500 film at (a) 800, (b) 900 and (c) 1000 °C annealing temperature for 1 h.

Fig. 5. Atomic structures of some planes of single crystal rutile TiO_2 and Ti.

also occurs in Ti-25 films [15]. This phenomenon can be ascribed as a result of the incorporation of oxygen atoms into the Ti structure. It is known that the thermal oxidation process of titanium is an oxygen diffusion-controlled mechanism [15–17]. Initially, a fast oxygen adsorption on titanium surface causes the formation of lower oxides after subsequently, oxygen molecules diffuse through the oxide layer into α-Ti. The maximum solubility of oxygen atoms in α-Ti can be reached to a level of O/Ti=0.5 mol% (i.e. oxygen-enriched Ti, where the oxygen atoms occupy the hole in every second layer of octahedral interstices, causing a considerable
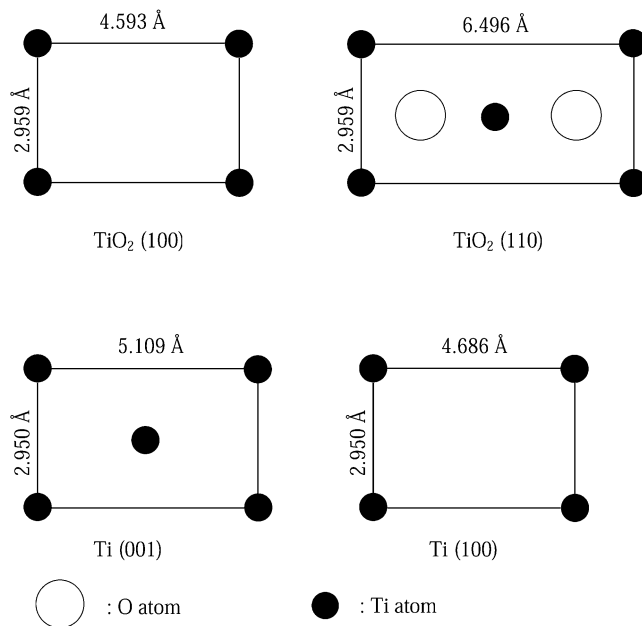
expansion in the c-axis, but only a slight change in the a-axis) [26]. Therefore, the structure of Ti films has changed to oxygen-enriched Ti (i.e. Ti_2O) before the rutile TiO_2 was detected by XRD, Fig. 6. After a complete transformation from Ti to TiO_2, the oxygen-enriched Ti_2O phase is acting as a crystallographic intermediate template and produces strain energy due to lattice misfits between Ti_2O and TiO_2 crystals

In general, a growing film has the tendency to reduce the overall film energy by minimizing the strain energy, due to lattice mismatch and surface free energy. For thermal oxidation of the amorphous and poorly crystalline Ti films (Ti-amorph and Ti-25), the XRD pattern
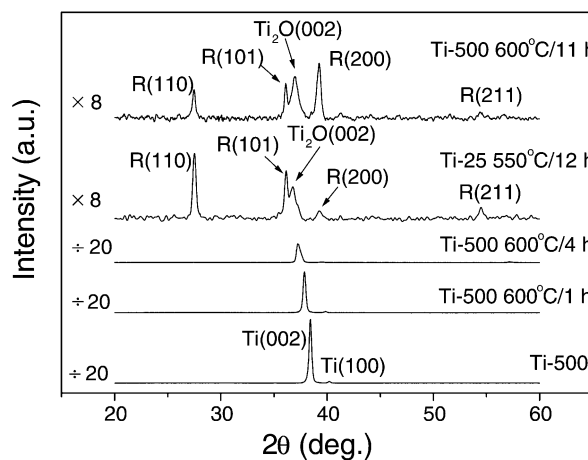

Fig. 6. XRD patterns of as-deposited Ti films with different sputtering condition after low temperature thermal oxidation.

Table 1
The integrated intensity ratios, $\gamma = I\,(200)/I\,(110)$, of the rutile TiO_2 films prepared under different oxidation temperatures for the Ti films deposited at different substrate temperatures

Oxidation temp. (°C)	$\gamma_{(Ti-25)}$	$\gamma_{(Ti-300)}$	$\gamma_{(Ti-500)}$
800	0.20	0.94	3.12
900	0.18	0.63	1.39
1000	0.11	0.60	1.15

Note that the $I\,(200)/I\,(110)$ ratio for randomly oriented TiO_2 crystals is 0.08.

of the resultant TiO_2 is similar to that of the powder TiO_2, having completely randomly oriented crystals. However, the TiO_2 from the well-crystalline Ti-500 film with stronger (002) preferred orientation exhibits a preferential growth along (200) orientation. These observations suggest that the development of preferred or randomly distributed rutile TiO_2 crystallites is strongly related to the crystallinity and orientation of initially-deposited Ti films. Although lattice mismatch between Ti_2O (001) and TiO_2 (100) is approximately 0.3% in the *a*-axis direction and 10% in the *c*-axis direction, a localized coherent relationship between Ti_2O and TiO_2 may exist, which further promotes the growth of TiO_2 with (200) orientation. From an energy viewpoint, strain energy can be minimized when (200)-oriented TiO_2 (relative to (110)-oriented TiO_2) developed on the (002)-oriented Ti crystallites whereupon the interfacial mismatch is optimized.

A higher temperature oxidation (> 900 °C) of Ti-500 films facilitates the formation of TiO_2 crystallites with random orientation, and the γ-value [the integrated intensity ratio of rutile $I\,(200)/I\,(110)$] decreased with increasing oxidation temperature, as shown in Table 1 and Fig. 3b. When oxygen atoms (5–24 at.%) dissolve in α-Ti, the structure of this oxygen-enriched Ti (i.e. hexagonal structure) can be stabilized at temperature as high as ∼1720 °C without changing to β-Ti [27]. However, at higher oxidation temperatures, the lattice vibration will further interfere with the local coherency between oxygen-enriched Ti and TiO_2, leading to the formation of randomly distributed TiO_2 crystallites. On the other hand, since the (110) plane has the lowest surface free energy, high-temperature oxidation seems favorable to bring the TiO_2 crystal growth towards a surface with the lowest surface free energy in order to reduce the overall energy. Additionally, by reducing the thickness of the Ti-500 film from 400 to 200 nm, a stronger rutile (200) peak appeared, resulting in an increased γ-value (8.39). The enhanced preferential growth toward (200) plane of thinner TiO_2 films can be attributed to reduced strain energy due to a decrease in film thickness [28].

4. Conclusion

Rutile TiO_2 films with random or (200) preferred orientations can be easily grown and tailored by the thermal oxidation of sputtered Ti metal films, having different degrees of crystallinity and preferred orientation. The preferential growth of TiO_2 film results from a competition between surface free energy effect and strain energy effect. The highly crystalline Ti film with (002) orientation can induce the preferential growth of the resultant TiO_2 crystals with (200) orientation. However, a randomly oriented rutile TiO_2 film is developed for the thermal oxidation of poorly crystalline Ti films. In addition, the preferential growth of (200)-oriented TiO_2 is enhanced by decreasing the film thickness where the strain energy is reduced. Higher temperature oxidation (≥ 900 °C) promotes the formation of rutile (110) plane because of surface free energy effect.

Acknowledgements

References

[1] H. Shibata, M. Murota, K. Hashimoto, Jpn. J. Appl. Phys. part 1 32 (1993) 4479.
[2] S. Veprek, Thin Solid Films 130 (1985) 135.
[3] E. Hecht, Optics, Addison-Wesley, 1987.
[4] L.J. Meng, M. Andritschky, M.P.d. Santos, Thin Solid Films 223 (1993) 242.
[5] F. Zhang, Z. Zheng, Y. Chen, D. Liu, X. Liu, J. Appl. Phys. 83 (1998) 4101.
[6] F. Zhan, X. Liu, Thin Solid Films 326 (1998) 171.
[7] U. Selvaraj, A.V. Prasadarao, S. Komarneni, R. Roy, J. Am. Ceram. Soc. 75 (1992) 1167.
[8] T. Fujii, N. Sakata, J. Takada, Y. Miura, Y. Daitoh, M. Takano, J. Mater. Res. 9 (1994) 1468.
[9] K.B. Alexander, F.J. Walker, R.A. McKee, F.A. III List, J. Am. Ceram. Soc. 73 (1990) 1737.
[10] W.W. Xu, R. Kershaw, K. Dwigh, A. Wold, Mater. Res. Bull. 25 (1990) 1385.
[11] M.H. Suhail, G.M. Rao, S. Mohan, J. Appl. Phys. 71 (1992) 1421.
[12] M. Radecka, K. Zakrzewska, H. Czternaste, T. Stapinski, Appl. Surf. Sci. 65/66 (1993) 227.
[13] W.G. Lee, S.I. Woo, J.C. Kim, S.H. Choi, K.H. Oh, Thin Solid Films 237 (1994) 105.
[14] T. Yoko, A. Yuasa, K. Kamiya, S. Sakka, J. Electrochem. Soc. 138 (1991) 2279.
[15] C.C. Ting, S.Y. Chen, D.M. Liu, J. Appl. Phys. 88 (2000) 4628.
[16] R. Padma, K. Ramkumar, M. Satyam, J. Mater. Sci. 23 (1988) 1591.
[17] J.W. Jr. Rogers, K.L. Erickson, D.N. Belton, R.W. Springer, T.N. Taylor, J.G. Beery, Appl. Surf. Sci. 35 (1989) 137.

[18] P. Kofstad, K. Hauffe, H. Kjöllesdal, Acta Chem. Scand. 11 (1957) 1641.

[19] ASTM JCPDS File No. 21-1276 (1997).

[20] H.M. Flower, P.R. Swann, Acta Met. 22 (1974) 1339.

[21] D.L. Douglass, J. Van Landuyt, Acta Met. 14 (1966) 491.

[22] R.A. Ploc, J. Nucl. Mater. 28 (1968) 48.

[23] K.R. Lawless, A.T. Gwathmey, Acta Met. 4 (1956) 153.

[24] N. Floquet, O. Bertrand, J.J. Heizmann, Oxid. Met. 37 (1992) 253.

[25] J.I. Eldridge, R.J. Hussey, D.F. Mitchell, M.J. Graham, Oxid. Met. 30 (1988) 301.

[26] B. Holmberg, Acta Chem. Scand. 16 (1962) 1245.

[27] J.L. Murray, Phase Diagrams of Binary Titanium Alloys, ASM International, USA, 1990, p. 212.

[28] J.E. Sundgren, Thin Solid Films 128 (1985) 21.